

Advanced Multilayer Cascade Multilayer Deep Neural Network Based Grid Integration of Hybrid PV and Wind Energy System



Mebrouk Mennad*, Bentaallah Abderrahim, Djeriri Youcef

ICEPS Laboratory (Intelligent Control & Electrical Power Systems), Engineer Sciences Faculty, Djillali Liabès University of Sidi Bel-Abbès, Sidi Bel-Abbès 22000, Algeria

Corresponding Author Email: mabroukmenad@gmail.com

<https://doi.org/10.18280/ejee.240101>

ABSTRACT

Received: 20 December 2020

Accepted: 20 December 2021

Keywords:

photovoltaic, wind, CFNN, power grid, fuzzy, indirect flux oriented control (IFOC)

An increasing number of industrialized and developing countries are concentrating their efforts in order to achieve net zero carbon emissions by generating electricity from renewable energy sources in the current environmental conditions. The Photovoltaic (PV) and wind energy systems have been modelled and their performance under a variety of operating situations has been investigated in this study work. Based on investigation the renewable energy sources are generate the nonlinear power under various weather conditions. Also, that the maximum power point tracking algorithm MPPT (P&O) play a major role for generate maximum power under the same conditions. The primary goal of this research project is to develop hybrid renewable energy system and integrated to microgrid power system and improve the power quality. To archive the primary goal to construct an advanced cascade feedforward deep neural network (CFNN) for the integration of hybrid solar and wind energy systems into the micro grid. The proposed controller will operate the grid integrated voltage source inverter for ensure real and reactive power flow through voltage source converter controller (Phase lock loop, Voltage regulator and current regulator). The proposed CFNN controller modelled for current regulator for improve the power quality and control real and reactive power flow. The proposed model has been created using the Math Works simulation environment as a starting point. The secondary goal of this project work is to develop battery management system for support excess power demand for consumer and store the power for future demand. and the simulated results are analyzed under a variety of operating scenarios, and the power quality results (THD for Voltage and Current) are evaluated and compared to industry standards, such as IEEE 519 standards. Finally, the effectiveness of the proposed system will be demonstrated.

1. INTRODUCTION

Microgrids, which make use of renewable and alternative energy technology, are now being used by customers to meet their energy demands while also helping to alleviate environmental problems in the process. As a result of the implementation of these modern technologies through a microgrid, resource efficiency is considerably improved, power quality is improved, and a more stable supply of energy is delivered. Grid advances such as multi-microgrids, interconnected AC-AC microgrids, and interconnected AC-DC microgrids, as well as zone-based and distributed grids, have enabled these newer characteristics to be integrated into grids that are zone-based or distributed. et cetera, Md. Halim Mondol is a professor at the University of Maryland. The half-height neutral point clamped (NPC) inverter is a modern single-phase multilevel inverter that has fewer switches than the previous generation inverters. One direct current source, one full bridge cell, switching devices, and half the number of power diodes seen in typical topologies are used in the proposed inverter [1].

Using a unipolar modulation technique, the switching signals for the proposed inverter are generated, resulting in the lowest total harmonic distortion (THD) in both the output

voltage and output current. Using the example of a single-phase eleven-level inverter, the inverter topology presented in this section is described. MATLAB/Simulink is used to simulate the topology. There is also a comparison between the proposed and traditional topologies. The following are the names of individuals: Md Mubashwar Hasan and others Numerous cascaded multilevel inverter (MLI) topologies that are unique to themselves have been proposed and published in the academic literature. All proposed topologies for three-phase cascaded MLI implementations have a fundamental disadvantage in that they require expensive semiconductor components and a high-voltage input dc supply [2]. This article presents a novel generalized concept that may be applied to any existing cascaded MLI topology in order to reduce the number of semiconductor switches, diodes, and dc power supply required for the system. The new generalized model is divided into two stages: a cascaded stage (CS) and a phase generator stage (PGS). In addition to a three-phase two-level inverter (CTPTLI) and three bidirectional (BD) switches, the PGS stage can be adjusted to accommodate any existing cascaded topology, although the cascaded stage cannot. Extensive modelling and experimental analysis are carried out in order to verify the proposed notion. Based on the findings, it appears that the proposed methodology can be used to

reduce the number of devices in existing topologies while maintaining their functionality.

Researchers Nakul Thombre and colleagues have developed a novel cascaded multilevel inverter design that allows for a significant decrease in the number of switches and DC voltage sources used. To achieve the desired output level, the proposed design is based on an asymmetrical multilevel inverter that contains eleven unidirectional switches, three diodes, and four direct current voltage sources to offer a total of 21 levels of output [3]. This topology has the advantage of lowering the number of switches and gate driver circuits (each with two), as well as the number of DC sources (each with two), that must be implemented (2 nos.) Furthermore, the hardware's cost, complexity, and physical space requirements are reduced without reducing the quality of the inverter's output, which is a significant benefit. C K Kishore and colleagues Instead of using clock phase shifting to regulate the cascaded switched diode (CSD) multilevel inverter, a sinusoidal pulse width modulation (SPWM) control technique was developed [4]. In the proposed cascaded switched diode multilevel inverter (CSDMLI) system, two identical resistive loads are connected to the inverter. When used in conjunction with multiple loads, the proposed MLI reduced harmonic content by up to 12.76 percent when compared to the existing control technique, which resulted in harmonic distortion of 16.82 percent. The transition between loads is accomplished by the use of a main pulse-width modulation technique. et cetera Mohammad Ali Hosseinzadeh is an Iranian politician. High-power medium-voltage applications benefit from the usage of multilevel inverters because they have reduced harmonics and a lower standing voltage on the power switches. The most significant disadvantage of multilayer inverters is that they need a large number of switching components, which makes control more difficult [5]. This work describes the design and fabrication of an asymmetric switch-diode multilevel inverter for use with cascaded multilevel inverters, as well as the operation of the device. Power switches and DC power sources are reduced in the proposed asymmetric multilevel inverter, which creates 31 levels with fewer power switches and DC power sources and a lower maximum total blocking voltage on the switches. A comparison is made between the proposed topology and other cascaded multilevel inverters in order to illustrate the advantages and disadvantages of multilevel inverters.

It is proposed in this paper to use a novel two-stage cascaded switched-diode multilevel inverter topology for the integration of medium voltage renewable energy. The fundamental goal of this design [6], is to reduce the number of switches and gate drivers on the circuit board. As a result, the installation space required for a multilayer inverter is reduced, as is the cost of installing one. Furthermore, by incorporating an artificial intelligence controller into multilevel inverters that are used for renewable energy integration, worries about dc source variations can be alleviated. Renewable and alternative energy sources can be used more efficiently with the help of these advanced network topologies, which is a significant plus for society. It is possible to connect two or more microgrids together to enable reserve sharing, voltage and frequency support, and ultimately boost the overall dependability and resilience of interconnected microgrids [7, 8].

The following is the structure of this paper. In Section II, the modelling of the PV and wind systems has been built, and the system's performance has been examined. Section III discusses the integration of hybrid PV and wind systems into the grid, as well as the design, performance, and comparisons

of the controllers. Section IV presents the findings of this study project as a conclusion.

2. MODELLING OF WIND AND PV SYSTEM

WECs with permanent magnet synchronous generators (PMFG) as their power source are widely used because research is continually identifying new designs that have high power density, higher efficiency, the possibility of smaller turbine diameters, and the availability of high-energy permanent magnet material at a reasonable price [9, 10]. A large number of research articles have been published in the development of WECS domain, with the goal of producing WECS that are more efficient, highly reliable, have minimal wear and tear, are quiet, are compact, and require less maintenance.

When converting variable voltage and variable frequency electricity to fixed frequency and fixed voltage power, the most common WECS configurations utilized with PMSG machines are three in number. A PMSG WECS with an appropriate MPPT controller is created and constructed for control of the converter, which is dependent on the converter configuration. For PMSG WECS, the MPPT controller algorithm is often implemented using one of three techniques.

The MPPT (maximum Power Point Tracking) controller is a control system for controlling the rotor speed of a wind turbine by manipulating the generating controlling torque generated by the turbine. The blade pitching drive causes a delay in response time with response to act proportionately with changes in wind conditions, such as turbulent and gusty winds, which has an impact on the energy yield and puts mechanical stress on the wind turbine as a result of this delay. On the other hand, the generator rotor speed can be regulated electrically in order to maximize the amount of electric power produced. The development of MPPT-based control approaches has been motivated by the goal of achieving the highest possible power coefficient [11]. The output power of a generator in a variable speed wind energy system is efficiently managed with the use of power electronics-based converters in a highly efficient manner.

The following is the proposed PMSG design parameter:

3000 watts of mechanical output power.

V_{max} is the maximum voltage that can be reached.

I_{max} is the maximum current available.

Base 2977.77 kilowatts of electrical generating power 12 m/s is the base wind speed.

1 p.u. is the rotational speed divided by the base.

Maximum power equals 0.8 p.u. at the base wind speed.

Pitch angle is equal to 0 degrees.

When using this P&O-based MPPT approach, the wind voltage and current are monitored in the current atmospheric conditions [12]. The wind power P1, which is determined by taking into account the tiny changes in duty cycle, and the wind power P2, which is computed by using the duty cycle. The wind power P2 is compared to the solar power P1. When P2 is greater than P1, the perturbation is considered valid; nonetheless, this approach has a significant drawback because of infrequent deviations from the maximum. A simulation of the modelled P&O based MPPT approaches for Wind systems has been built and tested in the Matlab environment, as illustrated in Figure 1. Figure 2 is represented 100 kW wind energy system simulation model. The wind energy system performance has been analyzed under various wind speed conditions as soon in Figure 3.

PO control Based MPPT Techniques for 30 KWatts Wind Power System

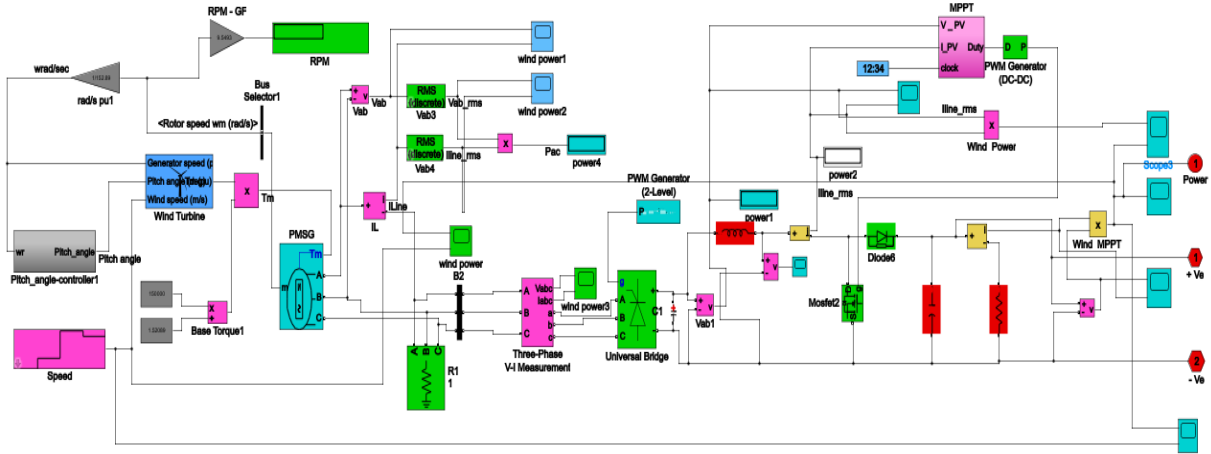


Figure 1. Matlab simulation model of winder energy system 30 kW

105 kW Wind Power system with MPPT controller and Fuzzy controller based Three phase grid connected inverter

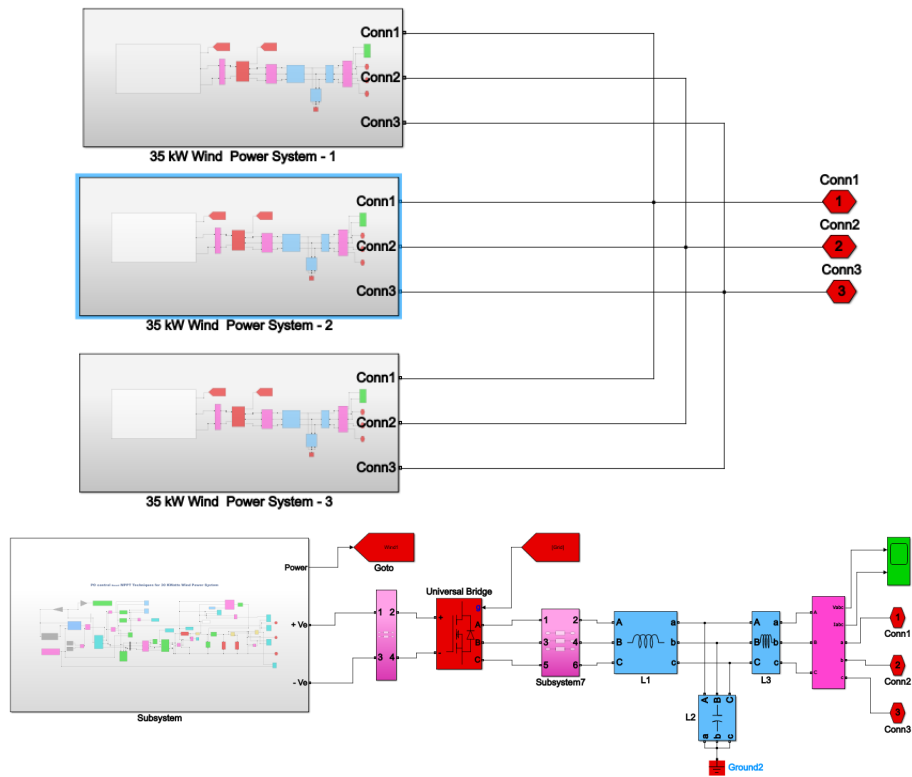


Figure 2. Matlab simulation model of winder energy system 100 kW

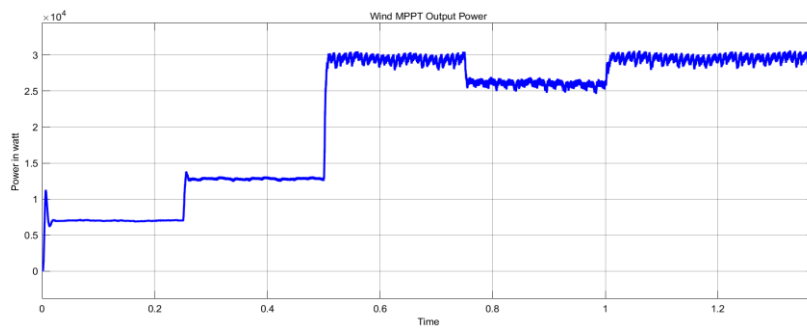


Figure 3. The wind energy system output power under various wind speed conditions

PV Simulation model

A significant role in meeting consumer electricity demand is played by renewable energy sources because of their abundant availability and low environmental impact. The most significant impediment to the growth of solar and wind energy is the high cost of putting solar and wind power systems in place [13, 14]. Because of the changing weather, solar and wind energy generation does not remain steady throughout the day. The efficiency of electricity generation is really low (the range of efficiency is only 9-17 percent in low irradiation regions). In order to achieve the best possible power output under a variety of weather circumstances, MPPT technologies play a vital role in PV and wind power generating.

PV voltage and current are monitored using this technology while the current atmospheric condition is maintained. PV power P_1 , which is estimated by taking into account the tiny changes in duty cycle, and PV power P_2 , which is also calculated. It is necessary to compare the PV power of P_2 with that of P_1 . When P_2 is greater than P_1 , the perturbation is considered valid; nonetheless, this approach has a significant drawback because of infrequent deviations from the maximum. As illustrated in Figure 4, the modelled P&O based MPPT approaches for PV systems have been created and tested in the Matlab environment. The 200 kW PV simulation model has been developed in MATLAB model as shown in Figure 5. Figures 6 & 7 illustrates the photovoltaic array out power generation under various weather conditions.

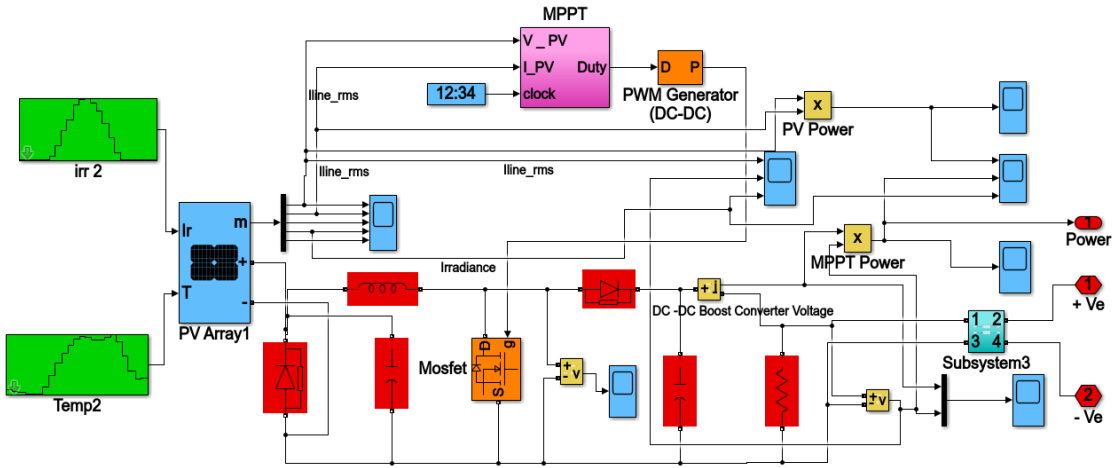


Figure 4. PV simulation model with MPPT controller

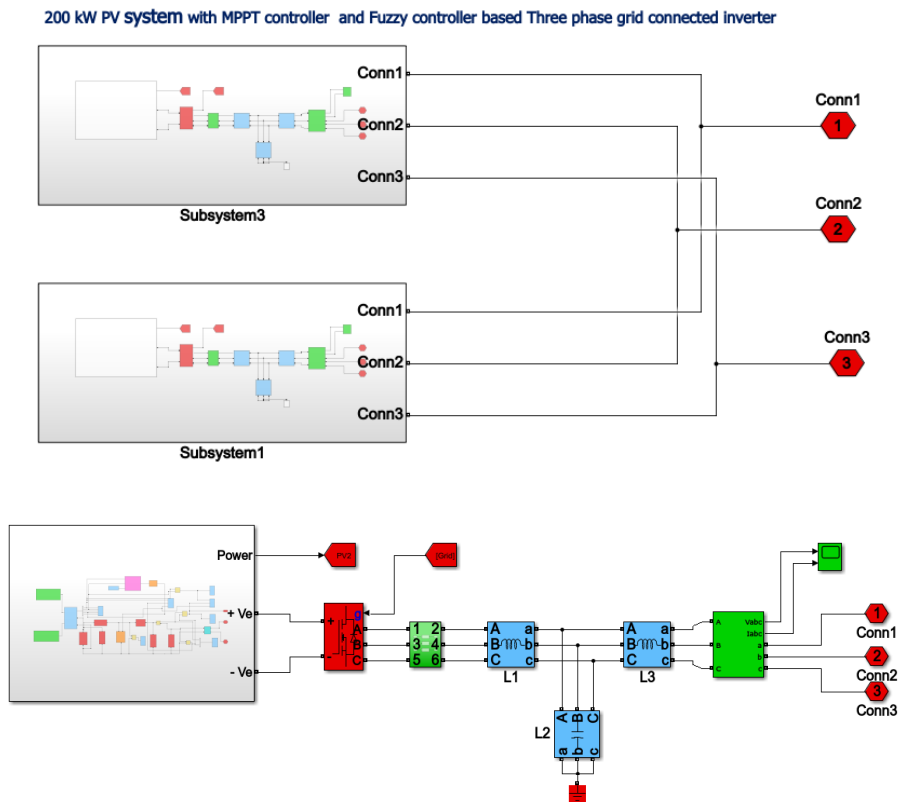


Figure 5. 200 kW PV simulation model

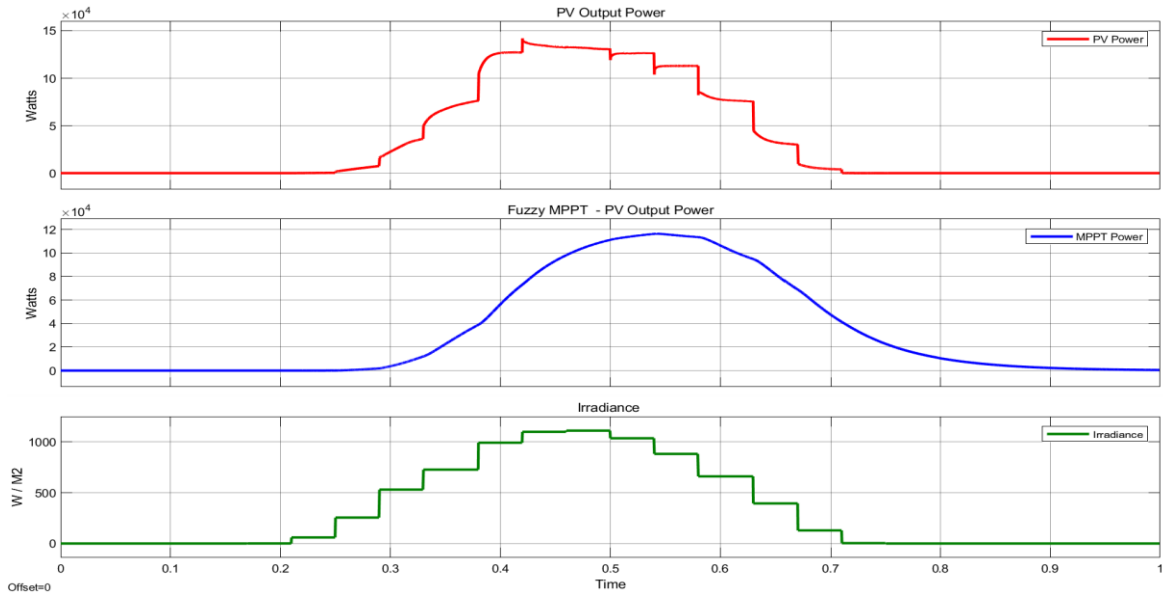


Figure 6. 100 kW PV system 1 simulation result under various weather conditions

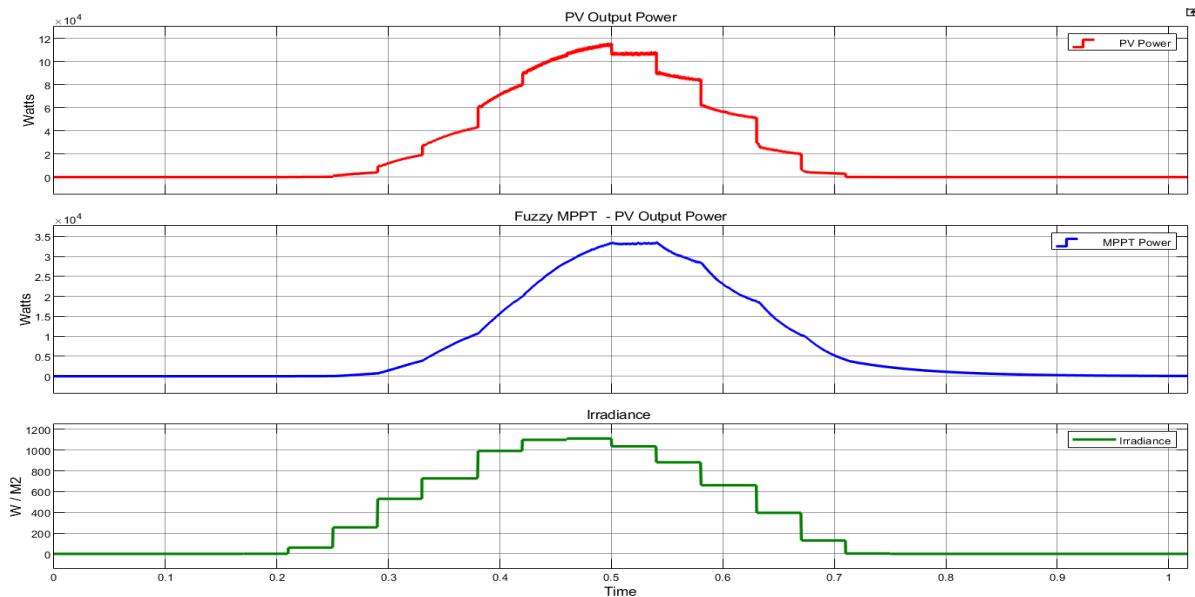


Figure 7. 100 kW PV system 2 simulation result under various weather conditions

PV voltage and current are monitored using this technology while the current atmospheric condition is maintained. PV power P1, which is estimated by taking into account the tiny changes in duty cycle, and PV power P2, which is also calculated. It is necessary to compare the PV power of P2 with that of P1. When P2 is greater than P1, the perturbation is considered valid; nonetheless, this approach has a significant drawback because of infrequent deviations from the maximum. As illustrated in Figure 1, the modelled P&O based MPPT approaches for PV systems have been created and tested in the Matlab environment. Figure 2 illustrates the voltage and current characteristics of a photovoltaic array.

3. GRID INTEGRATION OF HYBRID 300 KW PV / WIND ENERGY SYSTEM

Throughout this part, we have discussed the integration of a microgrid with a hybrid PV / wind-based power system, which has been created and regulated using a CFNN algorithm.

Figure 8 shows a detailed simulation model with a number of variables. This simulation model makes use of a hybrid PV and wind system of 300 kW. The wind energy system is linked into the power microgrid with the assistance of a smart inverter, which is controlled by a voltage source controller based on CFNN [15-17]. There are three key sub-controllers in this controller, which comprise a phase-lock loop, a current regulator, and a voltage regulator, among other things (Figure 9). In the end, the PWM signals are created by a current regulator that is connected to a smart inverter that is responsible for synchronizing a 300kW hybrid PV/wind and micro grid system. The phase lock loop model has been presented in Figure 10 and 11 shows voltage regulator. The CNFNN based current regulator has been presented in Figure 12, and the Figure 13 is CFNN network model.

In neural networks (NNs), the neuron is the fundamental building block. Neurons are connected by the weight of their synapses. Figure 4 depicts a neural network with five hidden layers and an output layer, which can be viewed. A Cascaded Feed Forward Neural Network is a type of neural network that

network that was built using this link design (CFNN). Alternatively, the equations of the CFNN model can be represented as follows:

$$y = \sum_{i=1}^n f^i w_i^j x_i + f^0 \left(\sum_{j=1}^k w_j^0 f_j^h \left(\sum_{j=1}^n w_{ji}^h x_i \right) \right) \quad (1)$$

As far as the activation function is concerned, that is the one between the input and output layers, and the weight in the input layer's activation function is the activation function from the input layer to the output layer. Eq. (2) becomes when an additional bias is applied to the input layer, and the activation function of each neuron in the hidden layer is f^h .

$$y = \sum_{i=1}^n f^i w_i^j x_i + f^0 \left(w^b + \sum_{j=1}^k w_j^0 f_j^h \left(\sum_{i=1}^n w_{ji}^h x_i \right) \right) \quad (2)$$

In most cases, time series data is employed in conjunction with the CFNN model. As a result, neurons in the input layer delay time series data represented by the data at the X_{t-1} , X_{t-2} , ..., X_{t-p} levels, and the output is the current data at the X_t level, as seen in the graph below. This link raises the predicted network weight, which leads the overall network size to increase by the number of neurons in the input layer, as seen in the graph below. It is divided into three stages: initial weight calculation, pattern error counting, and more weight computation. Backpropagation is a feedforward method based on convolutional neural networks. The error is determined during the feedforward phase, and then the process moves on to the next step, which is the feedforward calculation (the difference from the output to the target). The following step is to adjust the weights and then re-run the computation to confirm that everything is still accurate before proceeding. I was continuing to conduct this step as long as no errors or iteration halts were discovered during the process. The conjugate gradient optimization strategy for weighting modifications of the CFNN model is addressed in detail in this section, albeit only briefly. Assume that is a weight vector of length s and that the goal function is to find all of the network weights.

$$e = \frac{1}{2} (X_t - \hat{X}_t)^2 \quad (3)$$

Defined Q is the positive definite matrix of size $s \times s$ where $Q^T = Q$. Stages of the algorithm on Conjugate Gradient optimization are described as follows:

- Step 1: Set $k=0$, select the initial point $\Omega^{(0)}$;
- Step 2: Calculate the gradient of the initial weight:

$$g^{(0)} = \frac{\partial e}{\partial w^{(0)}} = \frac{\partial e}{\partial w} \Big|_{w=w^{(0)}} = \left[\frac{\partial e}{\partial w_1^{(0)}} \dots \frac{\partial e}{\partial w_s^{(0)}} \right]^T \quad (4)$$

If $g^{(0)}=0$ then stop, and it obtained the optimal weight $\Omega^{(0)}$. Else, set $d^{(0)}=g^{(0)}$.

- Step 3: Calculate

$$\alpha_k = \arg \min_{\alpha \geq 0} e(w^{(k)} + \alpha d^{(k)}) = - \frac{g^{(k)T} d^{(k)}}{d^{(k)T} Q d^{(k)}}$$

- Step 4: Calculate $\Omega^{(k+1)} = \Omega^{(k)} + \alpha_k d^{(k)}$.

- Step 5: $g^{(k+1)} = \frac{\partial e}{\partial w^{(k+1)}}$ if $g^{(k+1)} = 0$.

Stop and the optimal weight is $w^{(k+1)}$.

- Step 6: Calculate $\beta_k = \frac{g^{(k+1)T} Q d^{(k)}}{d^{(k)T} Q d^{(k)}}$.

- Step 7: $d^{(k+1)} = -g^{(k+1)} + \alpha_k d^{(k)}$.

- Step 8: $k=k+1$: go to step 3.

Epoch iteration in FFNN is commonly known as weight searching in the CFNN context. The program must not have met the iteration termination condition until the epoch $k=K$ in order to begin the iteration process at that point. Given that this strategy does not guarantee convergence in n steps, the direction vector is reset after each iteration, and the method is repeated until the termination condition is met [18, 19]. For each iteration of the nonlinear model, the nonlinear model calculates Q , which is a non-constant Hessian matrix. In order to keep the algorithm as simple as possible, an algorithm for eliminating Q is employed, with the result that the function and gradient value of each iteration remain the only sources of algorithm dependence throughout the algorithm. There are several formulas for substituting $Qd^{(k)}$ with other forms, such as the Hestenes-Stiefel formula, i.e. The form $Qd^{(k)}$ is replaced by $(g^{(k+1)} - g^{(k)})/\alpha_k$.

By this formula, the β_k becomes:

$$\beta_k = \frac{g^{(k+1)T} [g^{(k+1)} - g^{(k)}]}{d^{(k)T} [g^{(k+1)} - g^{(k)}]} \quad (5)$$

3.1 Result and discussion

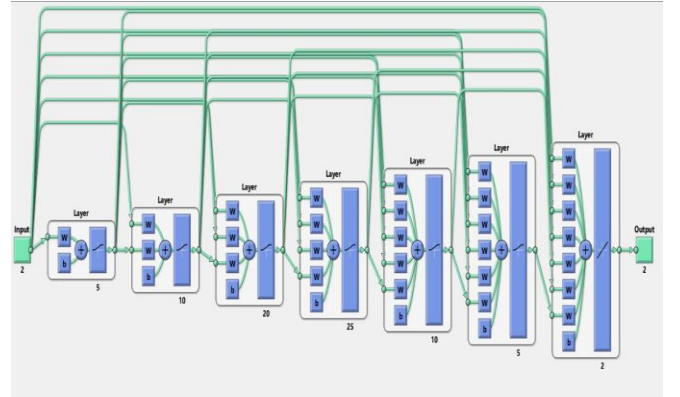


Figure 14. The cascade feed-forward neural network architecture

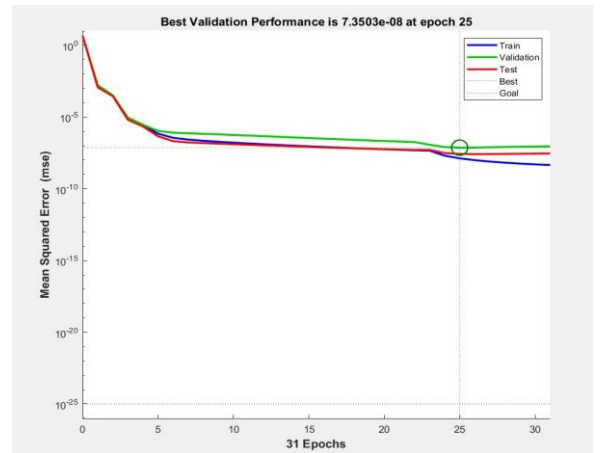


Figure 15. The best validation performance of CFNN model (7.3503e-8 at epoch 25)

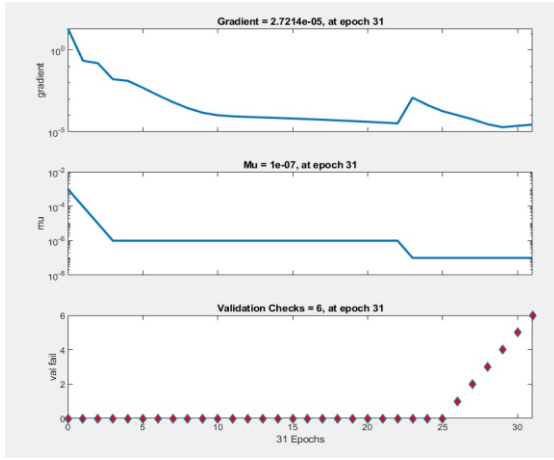


Figure 16. CFNN's Gradient, Mu, and validation checks for grid-connected VSC inverter current regulator

The suggested CFFNN-based algorithm has been constructed in the Matlab environment to demonstrate its functionality as shown in Figure 14. There are more than 90000 data points that are used for training (80 percent), testing (10 percent), and validation (the remaining 10 percent) (10 percent). As illustrated in Figure 15, the greatest validation performance of the proposed system is 7.3503×10^{-8} at epoch 25, which is the best possible value. As shown in Figure 16, the best validation performance of current regulation has been investigated using a variety of parameters such as gradient 2.7214×10^{-5} and $\mu 1 \times 10^{-7}$ at epoch 31 to determine the best validation performance. The overall performance of the suggested current regulator algorithms has been evaluated using the following parameters: training, validation testing, and overall results are shown in Figure 17. Figure 18 shows the overall results of the proposed current regulator algorithms. When the suggested multilayer inverter is synchronized with the electrical grid, the created current regulator algorithm is used to regulate the current flowing through it. The Figure 19 presented the bidirectional converter for battery system and its performance in Figure 20a. The results of the performance of

the three-phase induction machine are shown in Figure 20b, Despite the constraints of internal and external disturbances, and the importance of load demand of IM, and therefore the disadvantage of the sensitivity of the flux control (IFOC), following the high complicity of the nonlinearity of system, in particular that the unfavorable meteorological conditions of hybrid systems, the controller with deep artificial intelligence (CFNN) showed its robustness to convince the constraints of various global disturbances and ensures the perfect operation of control with this technique, which makes the synchronization operation and the interconnection between the hybrid networks and the load very satisfactory, and which meets the requirements of the ISO international energy standard and offers very favorable energy consumption rates.

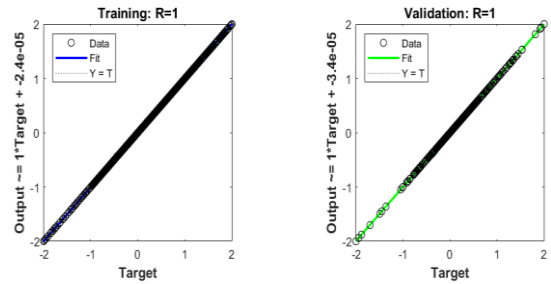


Figure 17. CFNN training and validation performance for grid-connected VSC inverter current regulator

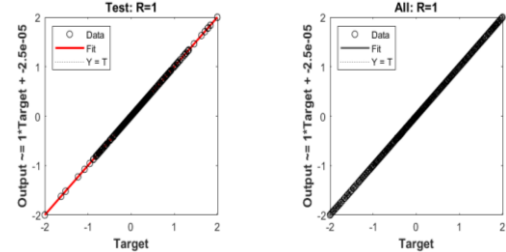


Figure 18. CFNN test and regression performance for grid-connected VSC inverter current regulator

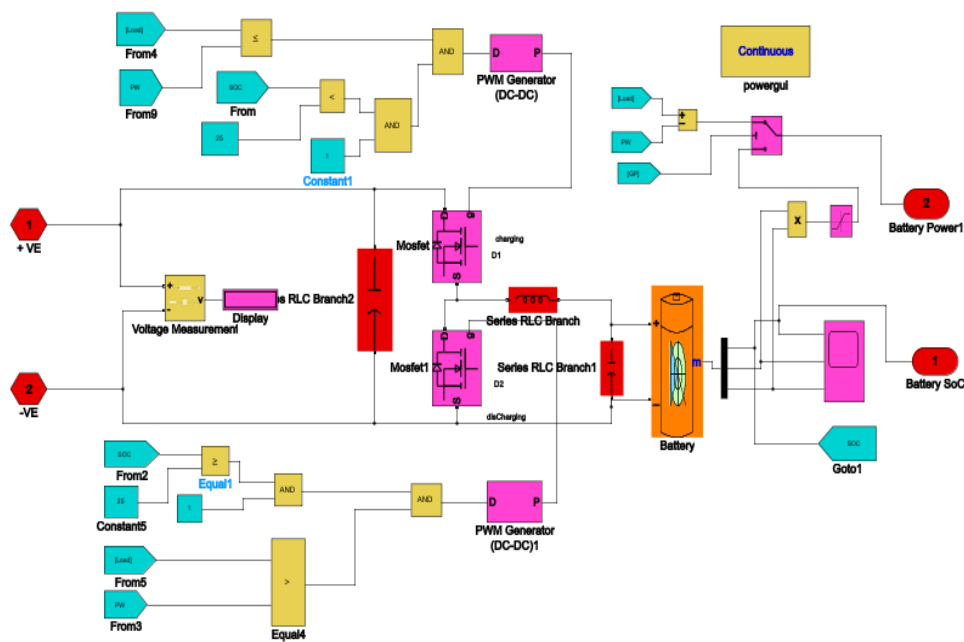
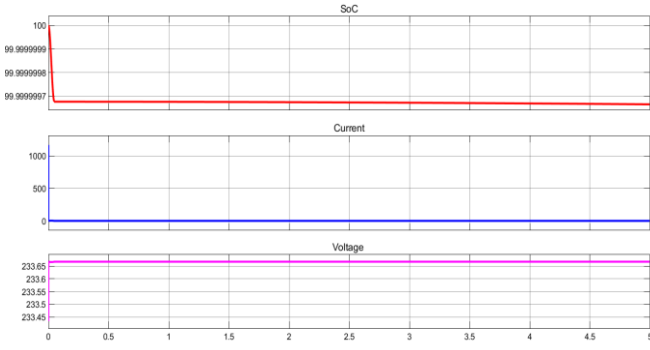
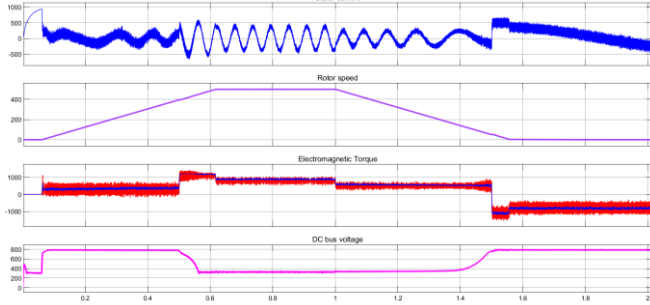


Figure 19. Bidirectional converter simulation model for battery energy management system



(a)



(b)

Figure 20. (a) Battery voltage, current and SoC; (b) Three Phase Induction motor performance under various conditions

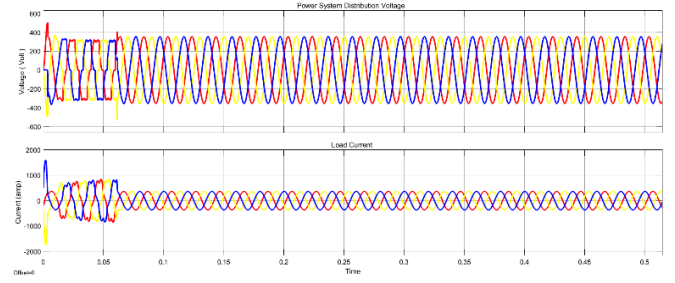


Figure 21. Grid distribution voltage and current waveform

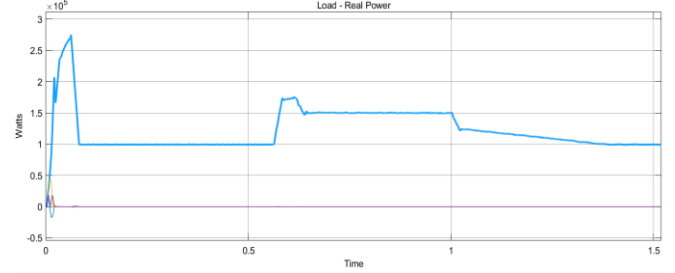


Figure 22. Real power simulation results

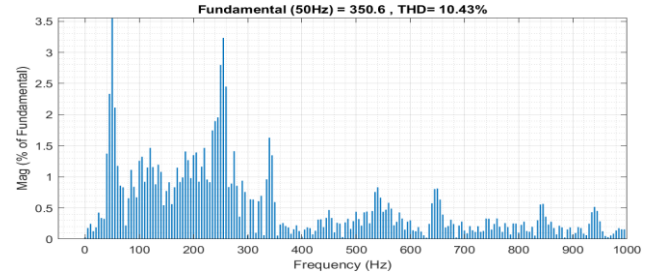


Figure 23. CFNN based distributed power grid voltage THD waveform (0 to 10 Cycle)

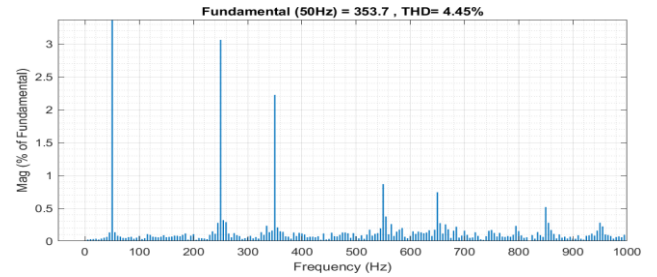


Figure 24. CFNN based distributed power grid voltage THD waveform after 1 sec (10 Cycle)

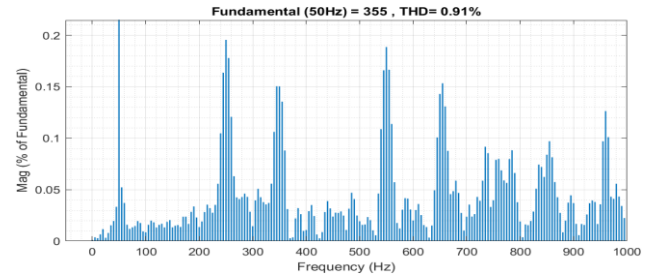


Figure 25. CFNN based distributed power grid voltage THD waveform after 1.3 sec (10 Cycle)

3.2 Results and discussion

Figure 21 depicts the voltage and waveform of a distributed power grid, whereas Figure 22 depicts a real-time power waveform. Figures 23 to 25 depicts the results of the THD assessments of the voltage profile performed using the CFNN algorithm. Figures 26 to 28 show THD analyses of the current profile performed using the CFNN THD analysis method. Figures 29, 30, and 31 show the fuzzy-based current regulator that was constructed in Matlab, as well as the rules-based system that was used to develop it. Figure 32 depicts a voltage and current waveform for a distribution power grid that is based on fuzzy logic. Figures 33 to 35 show the fuzzy based THD evaluations of the voltage profile, which are given in the same order. As seen in Figures 36 to 38, fuzzy THD evaluations of the current profile are provided in several ways. The voltage and current results for the fuzzy controller and the suggested controller are reported in Tables 1 and 2, respectively.

Table 1. Voltage THD comparison

THD	First 10 Cycle	After 1 sec (10 Cycle)	After 1.3 sec (10 Cycle)
CFNN	10.43%	4.45%	0.88%
Fuzzy	10.43%	4.45%	0.91%

Table 2. Current THD comparison

THD	First 10 Cycle	After 1 sec (10 Cycle)	After 1.3 sec (10 Cycle)
CFNN	26.96%	8.94%	1.49%
Fuzzy	26.96%	8.98%	1.50%

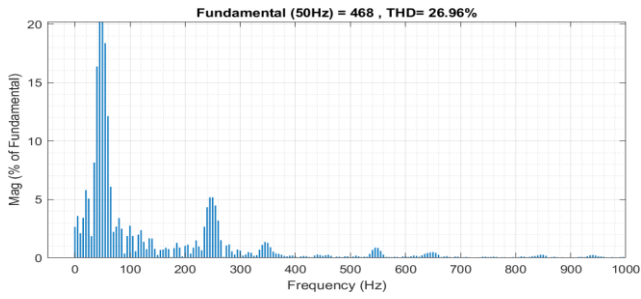


Figure 26. CFNN based distributed power grid load current THD waveform sec (0 to 10 Cycle)

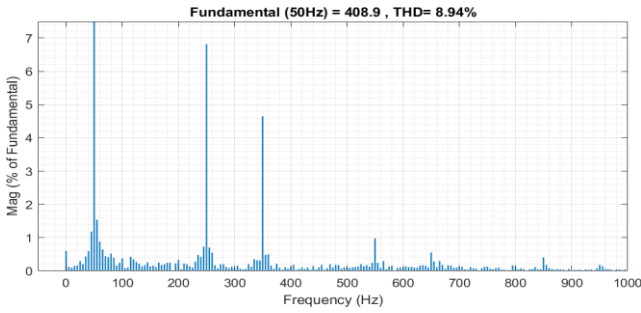


Figure 27. CFNN based distributed power grid load current THD waveform after 1 sec (0 to 10 Cycle)

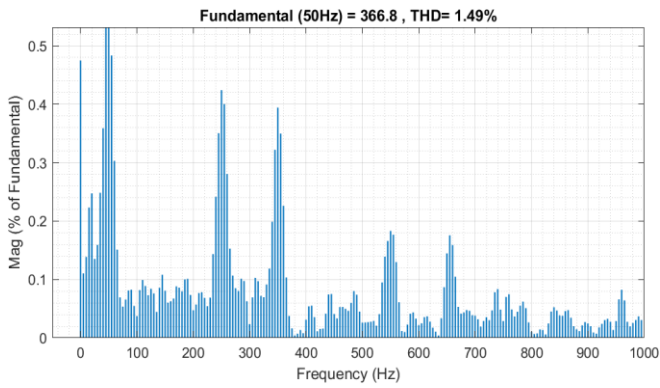


Figure 28. CFNN based distributed power grid load current THD waveform after 1.3 sec (0 to 10 Cycle)

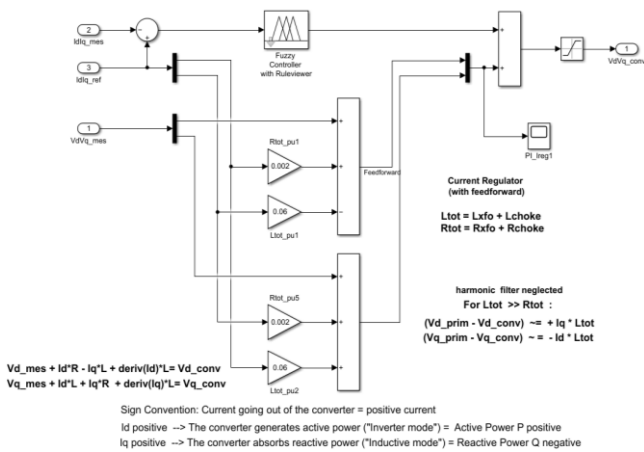


Figure 29. Fuzzy based current regulator

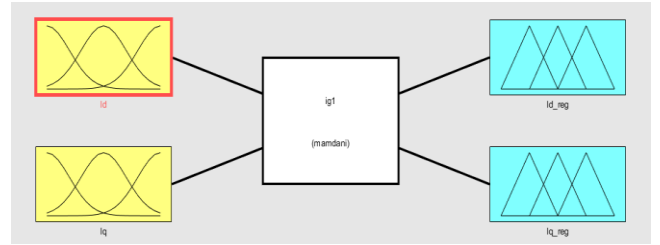


Figure 30. Fuzzy controller model for current regulator

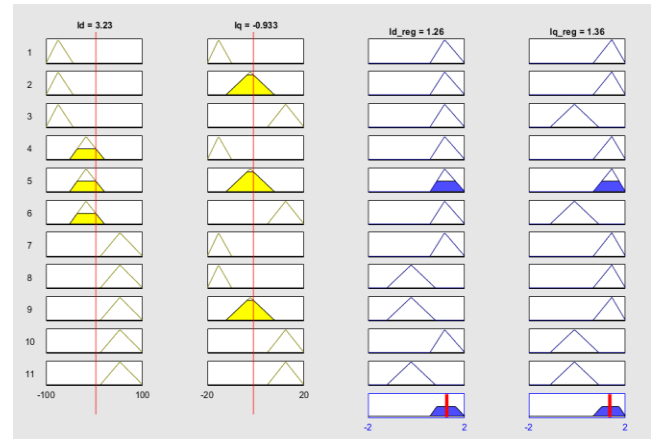


Figure 31. Fuzzy rules base system for current regulator

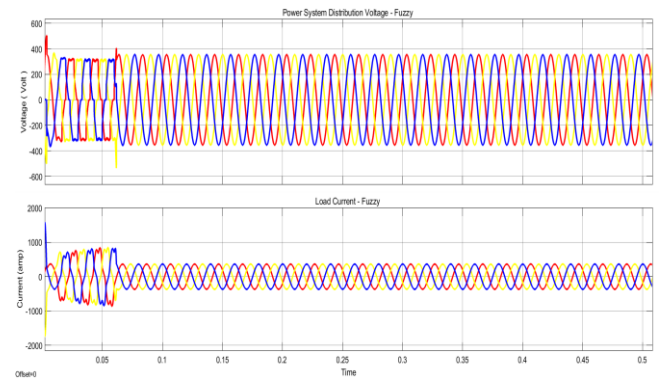


Figure 32. Fuzzy based distribution power grid voltage and current waveform

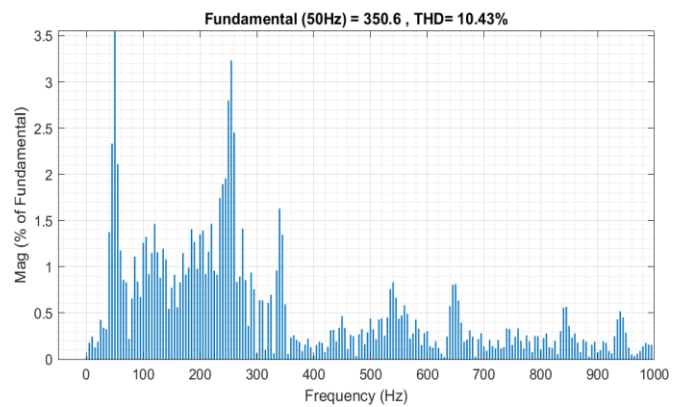


Figure 33. Fuzzy based distributed power grid voltage THD waveform (0 to 10 Cycle)

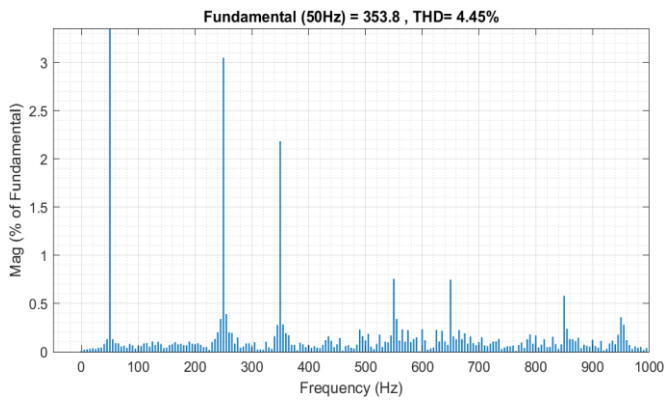


Figure 34. Fuzzy based distributed power grid voltage THD waveform after 1 sec (10 Cycle)

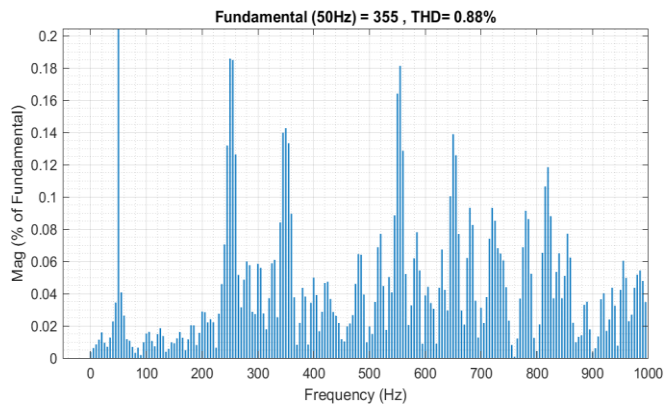


Figure 35. Fuzzy based distributed power grid voltage THD waveform after 1.3 sec (10 Cycle)

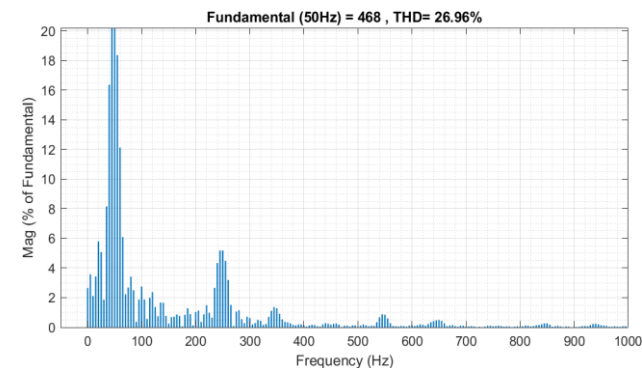


Figure 36. Fuzzy based distributed power grid load current THD waveform after 0 sec (10 Cycle)

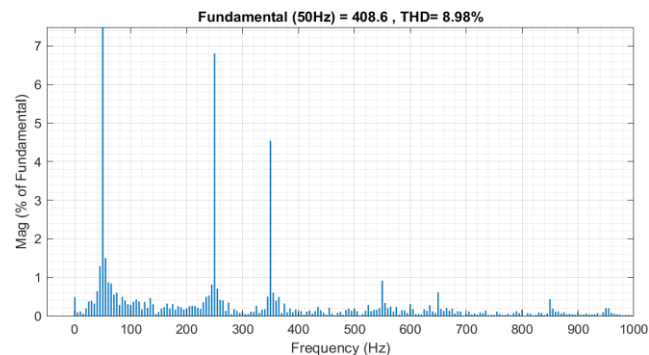


Figure 37. Fuzzy based distributed power grid load current THD waveform after 1 sec

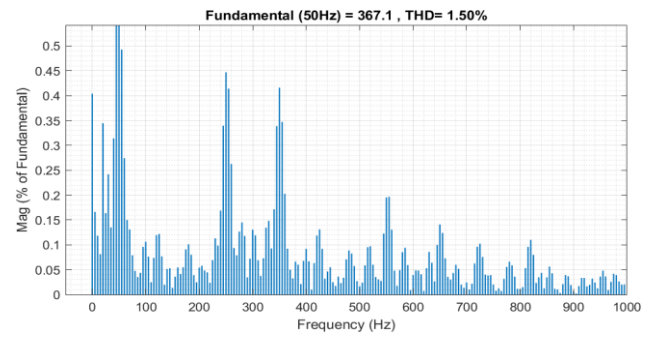


Figure 38. Fuzzy based distributed power grid load current THD waveform after 1.3 sec (0 to 10 Cycle)

4. CONCLUSIONS

This article concentrated on modeling the 300 kW PV system and implement it in Matlab. They have developed two-controller such as the CFNN algorithm and Fuzzy algorithm for the 200 kW PV and 100 kW wind system. The model was simulated, and the system's performance was assessed under various operating circumstances. The second section of this study report focused on photovoltaic system integration and performance. Finally, the suggested system was tested under various operating circumstances, and the findings are presented in Table 1 and Table 2. The effectiveness of the proposed system, simulation results are evaluated under IEEE 519.

REFERENCES

- [1] Mandol, M.H., Shuvra, P.B., Hosain, M.K., Samad, F., Rahman, M.W. (2019). A novel single phase multilevel inverter topology with reduced number of switching elements and optimum THD performance. In 2019 International Conference on Electrical, Computer and Communication Engineering (ECCE), Cox'sBazar, Bangladesh, pp. 1-5. <https://doi.org/10.1109/ECACE.2019.8679468>
- [2] Thombre, N., Singh Rawat, R., Rana, P., Umashankar, S. (2014). New cost effective cascaded twenty one level asymmetrical inverter with reduced number of switches and DC sources. In 2014 International Conference on Advances in Electrical Engineering (ICAEE), pp. 1-5. <https://doi.org/10.1109/ICAEE.2014.6838482>
- [3] Kishore, C.K., Balaji, K., Madhavan, J. (2019). Modified Cascaded switched diode multilevel inverter with multiple outputs and reduced harmonic content. In 2019 1st International Conference on Innovations in Information and Communication Technology (ICIICT), pp. 1-4. <https://doi.org/10.1109/ICIICT1.2019.8741436>
- [4] Hosseinzadeh, M.A., Sarbanzadeh, M., Rivera, M., Munoz, J., Villalon, A., Munoz, C. (2019). New single-phase asymmetric reduced multilevel inverter based on switched-diode for cascaded multilevel inverters. In 2019 IEEE International Conference on Industrial Technology (ICIT), pp. 1494-1499. <https://doi.org/10.1109/ICIT.2019.8755088>
- [5] Wang, L., Wu, Q.H., Tang, W. (2017). Novel cascaded switched-diode multilevel inverter for renewable energy integration. IEEE Transactions on Energy Conversion,

- 32(4): 1574-1582.
<https://doi.org/10.1109/TEC.2017.2710352>
- [6] Mohamed, M., Chandra, A., Abd, M.A., Singh, B. (2020). Application of machine learning for prediction of solar microgrid system. In 2020 IEEE International Conference on Power Electronics, Drives and Energy Systems (PEDES), pp. 1-5.
<https://doi.org/10.1109/PEDES49360.2020.9379497>
- [7] Abbasi, A., Karegar, H.K., Aghdam, T.S. (2020). Ensemble learning of decision trees for inverter-interfaced microgrid protection. In 2020 15th International Conference on Protection and Automation of Power Systems (IPAPS), pp. 136-139.
<https://doi.org/10.1109/IPAPS52181.2020.9375534>
- [8] Jayaraj, S., TP, I.A. (2019). Application of reinforcement learning algorithm for scheduling of microgrid. In 2019 Global Conference for Advancement in Technology (GCAT), pp. 1-5.
<https://doi.org/10.1109/GCAT47503.2019.8978453>
- [9] Wytock, M., Salapaka, S., Salapaka, M. (2014). Preventing cascading failures in microgrids with one-sided support vector machines. In 53rd IEEE Conference on Decision and Control, pp. 3252-3258.
<https://doi.org/10.1109/CDC.2014.7039892>
- [10] Dong, W., Yang, Q., Li, W., Zomaya, A.Y. (2021). Machine-learning-based real-time economic dispatch in islanding microgrids in a cloud-edge computing environment. *IEEE Internet of Things Journal*, 8(17): 13703-13711.
<https://doi.org/10.1109/JIOT.2021.3067951>
- [11] Roy, S., Nayar, S., Kumar, S., Alam, A., Ghose, T. (2019). Bidirectional power flow in DC microgrid and its islanding detection using support vector machine. In 2019 International Conference on Intelligent Computing and Control Systems (ICCS), pp. 42-47.
<https://doi.org/10.1109/ICCS45141.2019.9065548>
- [12] Venkateshkumar, M., Raghavan, R., Kumarappan, N. (2015). Design of a new multilevel inverter standalone hybrid PV/FC power system. *Fuel Cells*, 15(6): 862-875.
<https://doi.org/10.1002/fuce.201400085>
- [13] Venkateshkumar, M., Raghavan, R. (2015). Fuel cell power penetration into AC distribution grid by using new cascade multilevel inverter with minimum number of switches. In 2015 International Conference on Smart Technologies and Management for Computing, Communication, Controls, Energy and Materials (ICSTM), pp. 568-574.
<https://doi.org/10.1109/ICSTM.2015.7225480>
- [14] ELamin, M., Elhassan, F., Manzoul, M.A. (2021). Comparison of deep reinforcement learning algorithms in enhancing energy trading in microgrids. In 2020 International Conference on Computer, Control, Electrical, and Electronics Engineering (ICCCEEE), pp. 1-6.
<https://doi.org/10.1109/ICCCEEE49695.2021.9429565>
- [15] Lassetter, C., Cotilla-Sanchez, E., Kim, J. (2017). A learning scheme for microgrid reconnection. *IEEE Transactions on Power Systems*, 33(1): 691-700.
<https://doi.org/10.1109/TPWRS.2017.2709741>
- [16] Venkateshkumar, M., Indumathi, R. (2017). Comparative analysis of hybrid intelligent controller based MPPT of fuel cell power system. In 2017 IEEE International Conference on Smart Technologies and Management for Computing, Communication, Controls, Energy and Materials (ICSTM), pp. 155-159.
<https://doi.org/10.1109/ICSTM.2017.8089143>
- [17] Lakshmanan, S.A., Venkateshkumar, M. (2020). Analysis and design of lead-lag controller and fuzzy logic controller for boost converter applicable to RES. In 2020 International Conference on Power, Energy, Control and Transmission Systems (ICPECTS), pp. 1-6.
<https://doi.org/10.1109/ICPECTS49113.2020.9337004>
- [18] Chin, C.S., Xiao, J., Ghias, A.M., Venkateshkumar, M., Sauer, D.U. (2019). Customizable battery power system for marine and offshore applications: trends, configurations, and challenges. *IEEE Electrification Magazine*, 7(4): 46-55.
<https://doi.org/10.1109/MELE.2019.2943977>
- [19] Yu, J., Zhang, G., Peng, M., Song, D., Liu, M. (2020). Power-matching based SOC balancing method for cascaded H-bridge multilevel inverter. *CPSS Transactions on Power Electronics and Applications*, 5(4): 352-363.
<https://doi.org/10.24295/CPSSSTPEA.2020.00029>